



ARTICLE

AWK-TIS: An Improved AK-IS Based on Whale Optimization Algorithm and Truncated Importance Sampling for Reliability Analysis

Qiang Qin^{1,2,*}, Xiaolei Cao¹ and Shengpeng Zhang¹

¹Aerospace Science and Industry Corporation Defense Technology Research and Test Center, Beijing, 100854, China

²Key Laboratory for Thermal Science and Power Engineering of Ministry of Education, Department of Engineering Mechanics, Tsinghua University, Beijing, 100084, China

*Corresponding Author: Qiang Qin. Email: johnnystyle@126.com

Received: 20 February 2022 Accepted: 29 June 2022

ABSTRACT

In this work, an improved active kriging method based on the AK-IS and truncated importance sampling (TIS) method is proposed to efficiently evaluate structural reliability. The novel method called AWK-TIS is inspired by AK-IS and RBF-GA previously published in the literature. The innovation of the AWK-TIS is that TIS is adopted to lessen the sample pool size significantly, and the whale optimization algorithm (WOA) is employed to acquire the optimal Kriging model and the most probable point (MPP). To verify the performance of the AWK-TIS method for structural reliability, four numerical cases which are utilized as benchmarks in literature and one real engineering problem about a jet van manipulate mechanism are tested. The results indicate the accuracy and efficiency of the proposed method.

KEYWORDS

Structural reliability; active kriging; whale optimization algorithm; AK-IS

Nomenclature

AK	Active kriging
TIS	Truncated importance sampling
WOA	Whale optimization algorithm
MPP	Most probable point
MCS	Monte Carlo simulation
FORM	First order reliability method
SORM	Second order reliability method
LSF	Limit state function
RBF	Radial basis function
DOE	Design of experiment
ξ	Regression coefficient vector
$z(\mathbf{x})$	Stationary Gaussian process
σ_z^2	Process variance



$R(\mathbf{x}_i, \mathbf{x}_j)$	Correlation function
θ^*	Optimal correlation parameter
P_f	Failure probability
δ_{P_f}	Coefficient of variation of the failure probability
$\hat{G}(\mathbf{x})$	Limit state function constructed by kriging
λ	Positive penalty coefficient
ζ	Small constant
χ	Threshold
$x_i^{(t)}$	i -th search agent in the t -th iteration
$x_{best}^{(t)}$	The best agent in the t -th iteration
A_i	Random value
B_i	Random value
C_i	Random value
N_{IS}	Number of importance sampling
β	Reliability index

1 Introduction

Structural reliability analysis is often carried out to quantitatively assess the probability of structures' safe or failure state under the impact of uncertain factors in the environmental, structural and load parameters. Various structural reliability analysis methods, which can be broadly categorized into three main types: simulation-based methods, analytical methods or approximation methods, and meta-modeling methods, have been proposed over the past three decades [1,2].

Concerning simulation-based methods, the crude Monte Carlo simulation (MCS) method is the basic form of this classification, which evaluates the failure probability by dividing the number of samples falling into the failure domain by all the samples generated from the limit state evaluations. Although MCS is the most convenient implementation approach, it is extremely time-consuming when dealing with small failure probability and complex numerical models (e.g., fidelity finite element models (FEM)). Meanwhile, tremendous variation techniques of the MCS such as subset simulation [3,4], importance sampling [5,6] and directional sampling [7,8] have been developed to obtain more accurate results with fewer samplings. However, the main drawback of insufficient still exists in those methods.

As analytical methods, the traditional first-order and the second-order reliability methods (FORM and SORM) [9–12] respectively approximate the limit state function (LSF) around the most probable failure point (MPP) with first-order and incomplete second-order functions. The derivatives of the LSF with respect to the random variables have thus to be evaluated. Hence, these methods are not suitable for implicit limit state function and high nonlinearity cases.

Meta-modeling methods have been developed to balance the computational accuracy and efficiency during the structural reliability analysis, such as response surfaces [13–15], polynomial chaos expansion [16,17], artificial neural networks [18,19], support vector machine [20,21], radial basis function (RBF) [22,23] and Kriging metamodel [24,25]. In recent years, Kriging metamodel methods have obtained remarkable attention in the state-of-the-art literature. From the design of experiment (DOE) aspect of view, the strategy for constructing a Kriging model can broadly be classified into two sorts, the one is “one-shot” and the other is adaptive sampling or sequential sampling methods [26]. Literally, “one-shot” means producing enough design points before generating a Kriging model without supplementing new sample points in succeeding courses. Nevertheless, the adaptive sampling

methods generate a relatively small number of design points at the initial step, and then add one or more samples in each course of iteration according to certain regulations [27]. Furthermore, the exclusive feature of Kriging that it can predict the local uncertainty along with the prediction value promotes the development of the adaptive Kriging [24,28].

Two typical algorithms, the efficient global reliability analysis (EGRA) [28] and adaptive Kriging (AK) with MCS (AK-MCS) [29], are generously adopted and depict outstanding characters in diverse structural reliability problems. The amount of research has then further ameliorated the performance of active Kriging-based methods in recent years. These ameliorations resort to different and more efficient learning functions, sampling schemes and stopping criteria. Learning functions include the expected feasible function (*EFF*) [28], the learning function *U* [29], the learning function *H* [30], expected risk function (*ERF*) [31], least improvement function (*LIF*) [32], reliability-based expected improvement function (*REIF*) [33], Folded Normal based Expected Improvement Function (*FNEIF*) [34], K-means and weighted K-medoids algorithms-assisted learning process [35], and PDEM-oriented expected improvement function (*PEIF*) [36]. With regard to stopping criteria, it is common to see that when the values of learning functions reach certain thresholds the learning process stopped. For sampling tactics, importance sampling, subset simulation, line sampling, etc. have been adopted to evaluate failure probability in active Kriging (AK) reliability analysis, and some AK-based sampling methods were presented, such as AK-IS [37], AK-SS [38], AK-DS [39], AKOIS [40], AK-ARBIS [41], AK-SESC [42] and AKSE [43]. By combining these sampling methods with learning functions, the number of calls of limit state functions has reduced dramatically with acceptable accuracy of variation coefficient of failure probability. Despite the aforementioned learning functions, the correlation parameter θ also plays a vital role in constructing an accurate Kriging model. Thus, the pattern search algorithm is applied in DACE to calculate the optimum of θ [44]. However, as a local optimization algorithm, pattern search is sensitive to the initial value and may get trapped in local optimum. Then, various global optimization algorithms, such as genetic algorithm (GA) [33,45], DIRECT algorithm [46], particle swarm optimization (PSO) [47], and artificial bee colony (ABC) [48], are adopted to find the optimal value of θ by solving the maximum likelihood equation. Compared with GA, PSO, and the pattern search, the whale optimization algorithm (WOA) [49] proposed in the year of 2016 has its own advantages, such as simple principle, easy implementation, high convergence speed and calculation accuracy.

This paper aims to improve the efficiency and accuracy of the AK-IS for structural reliability analysis. In this paper, AWK-TIS is proposed, which is inspired by AK-IS [34] and RBF-GA [50], coupling with WOA and Truncated importance sampling (TIS) [51,52], and the WOA in AWK-TIS is adopted to seek the optimum of correlation parameter θ and the MPP in different phases of each course of iterations. Moreover, inside of the optimal β -sphere treated as the safe state, the samples are eliminated by TIS. Therefore, the prediction of Kriging model and the selection of the best next sample are only implemented through the candidate samples outside the optimal β -sphere, which significantly reduces the computational time and saves computer memory in comparison with the original AK-IS.

The remainder of the manuscript is organized as follows. Section 2 briefly introduces the Kriging method, AK-IS method, TIS and WOA. In Section 3, the procedures and the main steps of the AWK-TIS method are proposed. In Section 4, the applicability of the proposed technique is validated by four numerical cases and one real engineering problem of jet van manipulation mechanism. Finally, conclusions are summarized in Section 5.

2 Backgrounds

Before introducing the proposed AWK-TIS algorithm, some basic theories are briefly recalled, e.g., the Kriging method, the main steps of the AK-IS algorithm and truncated importance sampling (TIS) method, and the WOA.

2.1 Basic Theory about Kriging Method

Kriging metamodel, which consists of a parametric linear regression model and a nonparametric stochastic process, is an interpolation technique based on statistical theory. It needs a DOEs to determine its stochastic parameters and then predictions of the response can be inferred on any unknown point. Give a set of initial DOEs $\mathbf{X} = [\mathbf{x}_1, \mathbf{x}_2, \dots, \mathbf{x}_m]$, with $\mathbf{x}_i \in \mathbb{R}^n (i = 1, 2, \dots, m)$ the i th experiment, and $\mathbf{G} = [G(\mathbf{x}_1), G(\mathbf{x}_2), \dots, G(\mathbf{x}_m)]$ is the corresponding response to \mathbf{X} . The approximate relationship between any experiment \mathbf{x} and the response $G(\mathbf{x})$ can be denoted as [41,42]:

$$\hat{G}(\mathbf{x}) = \mathbf{F}(\boldsymbol{\xi}, \mathbf{x}) + z(\mathbf{x}) = \mathbf{f}^T(\mathbf{x}) \boldsymbol{\xi} + z(\mathbf{x}) \quad (1)$$

where $\boldsymbol{\xi}^T = [\xi_1, \dots, \xi_p]$ is a regression coefficient vector, $\mathbf{f}^T(\mathbf{x}) = [f_1(\mathbf{x}), f_2(\mathbf{x}), \dots, f_p(\mathbf{x})]^T$ is the basic functions vector which makes a global simulation in design space. In the ordinary Kriging, $\mathbf{F}(\boldsymbol{\xi}, \mathbf{x})$ is a scalar and always taken as $\mathbf{F}(\boldsymbol{\xi}, \mathbf{x}) = \boldsymbol{\xi}$; $z(\mathbf{x})$ is a stationary Gaussian process with zero mean and covariance between two data points \mathbf{x}_i and \mathbf{x}_j is denoted as:

$$\text{Cov}[z(\mathbf{x}_i), z(\mathbf{x}_j)] = \sigma_z^2 R(\mathbf{x}_i, \mathbf{x}_j) \quad (2)$$

where σ_z^2 is the process variance, and $\mathbf{x}_i, \mathbf{x}_j$ are data points from the whole samples \mathbf{X} . $R(\mathbf{x}_i, \mathbf{x}_j)$ is the correlation function about \mathbf{x}_i and \mathbf{x}_j with a correlation parameter vector $\boldsymbol{\theta}$ that has to be estimated by pattern search method in DACE. A diversity of models can be adopted to define correlation function $R(\mathbf{x}_i, \mathbf{x}_j)$, such as Gaussian correlative model, experimental and linear model, etc. The widely employed Gaussian model is accepted in the paper and can be defined as:

$$R(\mathbf{x}_i, \mathbf{x}_j) = \exp \sum_{k=1}^n \left[-\theta_k (\mathbf{x}_i^k - \mathbf{x}_j^k)^2 \right] \quad \theta_k \geq 0 \quad (3)$$

where n is the dimension of the sample, $\mathbf{x}_i^k, \mathbf{x}_j^k$ and θ_k are the k th components of data sample $\mathbf{x}_i, \mathbf{x}_j$ and $\boldsymbol{\theta}$, respectively.

Define correlation matrix $\mathbf{R} = [R(\mathbf{x}_i, \mathbf{x}_j)]_{m \times m}$, \mathbf{F} is a $m \times 1$ unit vector, then $\boldsymbol{\xi}$ and σ_z^2 are given by:

$$\hat{\boldsymbol{\xi}} = (\mathbf{F}^T \mathbf{R}^{-1} \mathbf{F})^{-1} \mathbf{F}^T \mathbf{R}^{-1} \mathbf{G} \quad (4)$$

$$\hat{\sigma}_z^2 = (\mathbf{G} - \hat{\boldsymbol{\xi}} \mathbf{F})^T \mathbf{R}^{-1} (\mathbf{G} - \hat{\boldsymbol{\xi}} \mathbf{F}) / m \quad (5)$$

where $\mathbf{R}, \hat{\boldsymbol{\xi}}$ and $\hat{\sigma}_z^2$ are functions of $\boldsymbol{\theta}$.

Then at an unknown point \mathbf{x} , the Best Linear Unbiased Predictor (BLUP) of the response $\hat{G}(\mathbf{x})$ is shown to be a Gaussian random variant $\hat{G}(\mathbf{x}) \sim N(\mu_{\hat{G}}(\mathbf{x}), \sigma_{\hat{G}}^2(\mathbf{x}))$, where

$$\mu_{\hat{G}}(\mathbf{x}) = \hat{\boldsymbol{\xi}} + \mathbf{r}(\mathbf{x}) \mathbf{R}^{-1} (\mathbf{G} - \hat{\boldsymbol{\xi}} \mathbf{F}) \quad (6)$$

$$\sigma_{\hat{G}}^2(\mathbf{x}) = \sigma_z^2(\mathbf{x}) \left(1 + \mathbf{v}^T(\mathbf{x}) (\mathbf{F}^T \mathbf{R}^{-1} \mathbf{F})^{-1} \mathbf{v}(\mathbf{x}) - \mathbf{r}^T(\mathbf{x}) \mathbf{R}^{-1} \mathbf{r}(\mathbf{x}) \right) \quad (7)$$

where $\mathbf{r}(\mathbf{x}) = [R(\mathbf{x}, \mathbf{x}_1), R(\mathbf{x}, \mathbf{x}_2), \dots, R(\mathbf{x}, \mathbf{x}_m)]$, $\mathbf{v}(\mathbf{x}) = \mathbf{F}^T \mathbf{R}^{-1} \mathbf{r}(\mathbf{x}) - 1$. $\mu_{\hat{G}}(\mathbf{x})$ is usually taken as the estimated $\hat{G}(\mathbf{x})$ at point \mathbf{x} . That means Kriging is an exact interpolation method.

The correlation parameter θ can be obtained through the maximum likelihood estimation (MLE) [47,48]:

$$\theta = \arg \min \varphi(\theta) = \arg \min (m \ln \hat{\sigma}_z^2 + \ln |\mathbf{R}|) \tag{8}$$

where $|\mathbf{R}|$ is the determinant of \mathbf{R} . The optimal Kriging model can be obtained if the optimal correlation parameter θ^* is guaranteed. The Eq. (8) can be solved by pattern search method, genetic algorithm, PSO, etc. It should be noted that since the introduction of WOA, this algorithm has been used in many fields and showed its superiority over many other metaheuristic algorithms such as PSO, ABC, GA, etc. As a result, WOA is adopted to search θ^* in this study.

2.2 AK-IS Algorithm

AK-IS mainly consists of two steps. The first step is the FORM approximation, which is utilized to find the MPP that is not accurate enough to evaluate the probability. The second step is to establish an AK model with a special learning function and stopping criteria to reduce the calls of original limit state function. In this step, IS method is adopted to calculate the failure probability and its coefficient of variation.

IS requires the definition of a joint PDF φ_n that is taken as a standard Gaussian one centered at the MPP found in the first step for the new sampling. The failure probability is estimated as [37]:

$$P_f = \int_{\mathbb{R}^n} I_F(\mathbf{u}) \frac{\phi_n(\mathbf{u})}{\varphi_n(\mathbf{u})} \varphi_n(\mathbf{u}) du_1 \cdots du_n \tag{9}$$

where $I_F(\mathbf{u})$ is indicator function, $I_F(\mathbf{u}) = \{0 \text{ if } G(\mathbf{u}) > 0 \text{ and } 1 \text{ if } G(\mathbf{u}) \leq 0\}$.

A number of N_{IS} samples denoted $\{\tilde{\mathbf{u}}^{(i)}, i = 1, \dots, N_{IS}\}$ are generated according to importance sampling density function φ_n . The integral is then expressed by:

$$P_f \approx \hat{P}_{f,IS} = \frac{1}{N_{IS}} \sum_{i=1}^{N_{IS}} I_F(\tilde{\mathbf{u}}^{(i)}) \frac{\phi_n(\tilde{\mathbf{u}}^{(i)})}{\varphi_n(\tilde{\mathbf{u}}^{(i)})} \tag{10}$$

The variance of the failure probability estimator is given as:

$$\text{Var}[\hat{P}_{f,IS}] = \frac{1}{N_{IS}} \left(\frac{1}{N_{IS}} \sum_{i=1}^{N_{IS}} \left(I_F(\tilde{\mathbf{u}}^{(i)}) \left(\frac{\phi_n(\tilde{\mathbf{u}}^{(i)})}{\varphi_n(\tilde{\mathbf{u}}^{(i)})} \right)^2 \right) - \hat{P}_{f,IS}^2 \right) \tag{11}$$

The coefficient of variation δ_{IS} of the failure probability estimator is then:

$$\delta_{IS} = \sqrt{\frac{\text{Var}[\hat{P}_{f,IS}]}{\hat{P}_{f,IS}}} \tag{12}$$

Besides, the learning function U proposed in AK-MCS is still used in AK-IS:

$$U(\mathbf{x}) = \frac{|\mu_{\hat{G}}(\mathbf{x})|}{\sigma_{\hat{G}}(\mathbf{x})} \tag{13}$$

where $\mu_{\hat{G}}(\mathbf{x})$ and $\sigma_{\hat{G}}(\mathbf{x})$ are Kriging mean and standard deviation, respectively. Moreover, the sample that has the minimum of $U(\mathbf{x})$ is called the best next sample and it is iteratively enriched the DOE to update the Kriging model. The learning process stops if the minimum of the learning function U is larger than its threshold. Besides, the active procedure continues and N_{IS} new samples are enlarged until the coefficient of variation δ_{IS} is smaller than a limit value which is set to 0.05 in AK-IS.

2.3 Truncated Importance Sampling

Truncated importance sampling (TIS) method is developed by introducing a hypersphere with the radial, which is indicated by β shown in Fig. 1, equals to the minimum distance from the origin to the limit state surface in \mathbf{u} -space [51,52].

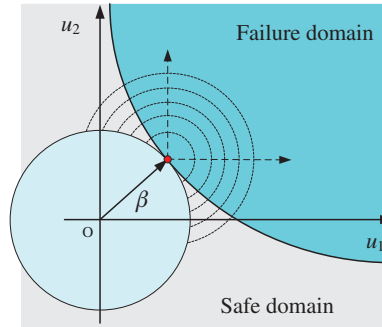


Figure 1: Sketch of TIS

The red point in Fig. 1 indicates the MPP.

The indicator function of the outer of the β -sphere is defined as follows:

$$I_{\beta}(\tilde{\mathbf{u}}^{(i)}) = \begin{cases} 0 & \text{if } \|\tilde{\mathbf{u}}^{(i)}\|^2 \leq \beta^2 \\ 1 & \text{if } \|\tilde{\mathbf{u}}^{(i)}\|^2 > \beta^2 \end{cases} \quad (14)$$

where the inner of the β -sphere contains part of the safe domain or even all of the district, while other domains including all the failure domain and part of the safe domain are out of the β -sphere. It can be seen that the indicator function I_F of the samples located in the β -sphere is $I_F(\tilde{\mathbf{u}}) = 0$, and there is unnecessary to call the true model to evaluate whether safe or not. The integral is then estimated by:

$$P_f \approx \hat{P}_{f,TIS} = \frac{1}{N_{IS}} \sum_{i=1}^{N_{IS}} \frac{I_F(\tilde{\mathbf{u}}^{(i)}) I_{\beta}(\tilde{\mathbf{u}}^{(i)}) \phi_n(\tilde{\mathbf{u}}^{(i)})}{\varphi_n(\tilde{\mathbf{u}}^{(i)})} \quad (15)$$

The variance of the failure probability estimator is estimated as:

$$\text{Var}[\hat{P}_{f,TIS}] = \frac{1}{N_{IS} - 1} \left(\frac{1}{N_{IS}} \sum_{i=1}^{N_{IS}} \left(I_F(\tilde{\mathbf{u}}^{(i)}) I_{\beta}(\tilde{\mathbf{u}}^{(i)}) \left(\frac{\phi_n(\tilde{\mathbf{u}}^{(i)})}{\varphi_n(\tilde{\mathbf{u}}^{(i)})} \right)^2 \right) - \hat{P}_{f,TIS}^2 \right) \quad (16)$$

The coefficient of variation (C.O.V) δ_{TIS} of the failure probability estimator is then:

$$\delta_{TIS} = \sqrt{\frac{\text{Var}[\hat{P}_{f,TIS}]}{\hat{P}_{f,TIS}}} \quad (17)$$

2.4 Whale Optimization Algorithm

The Whale Optimization Algorithm (WOA) is a novel nature-inspired population-based meta-heuristic algorithm, presented by Seyedali Mirjalili and Andrew Lewis from Griffith University in 2016 [49]. It was abstracted from the special hunting behavior of humpback whales. This foraging behavior is named bubble-net feeding method.

Two approaches namely, shrinking encircling mechanism and spiral updating position, are designed to mathematically model the exploitation phase of the WOA. The first approach is formulated as follows:

$$x_i^{(t+1)} = x_{best}^{(t)} - A_i \cdot |C_i \cdot x_{best}^{(t)} - x_i^{(t)}| \tag{18}$$

where t indicates the current iteration, A_i and C_i are coefficients. $x_i^{(t)}$ and $x_{best}^{(t)}$ represent i -th search agent and the best agent in the t -th iteration, respectively.

$$A_i = 2q \cdot r_{i1} - q \tag{19}$$

$$C_i = 2r_{i2} \tag{20}$$

where q is linearly reduced from 2 to 0 over the course of iterations, r_{i1} , r_{i2} are random numbers in $[0, 1]$. A_i is a random value in the interval $[-2q, 2q]$. When the random value of A_i is in $[-1, 1]$, the next position of a search agent can be in any position of the agent and the position of the current best agent. The parameter C_i is a random value in $[0, 2]$. This component provides random weights for prey in order to stochastically emphasize ($C_i > 1$) or deemphasize ($C_i < 1$) the effect of prey in defining the distance between the search agent and the current best agent. Besides, the second approach, the process of spiral updating position, is expressed as follows:

$$x_i^{(t+1)} = x_{best}^{(t)} + |x_{best}^{(t)} - x_i^{(t)}| \cdot e^{bl} \cdot \cos(2\pi l) \tag{21}$$

where b is a constant for defining the ‘9’-shaped path of distinctive bubbles created by the humpback whales, l is a random number in $[-1, 1]$.

The humpback whales hunt the prey by using the shrinking circle mechanism and spiral updating method simultaneously, and the two approaches have the same possibility to be chosen, so the model of the exploitation phase is as follows:

$$x_i^{(t+1)} = \begin{cases} x_{best}^{(t)} - A_i \cdot |C_i \cdot x_{best}^{(t)} - x_i^{(t)}| & \text{if } r_{i3} < 0.5 \\ x_{best}^{(t)} + |x_{best}^{(t)} - x_i^{(t)}| \cdot e^{bl} \cdot \cos(2\pi l) & \text{if } r_{i3} \geq 0.5 \end{cases} \tag{22}$$

where r_{i3} are random numbers in $[0, 1]$ to switch the different mathematical model of exploitation.

However, the process of search for prey is defined as the exploration phase, and the model of this phase is described as follows:

$$x_i^{(t+1)} = x_j^{(t)} - A_i \cdot |C_i \cdot x_j^{(t)} - x_i^{(t)}| \tag{23}$$

where $x_j^{(t)}$ is the j -th random search agent which is different from the $x_i^{(t)}$, and A_i is also defined by Eq. (19), but it is absolute value, $|A_i|$, is greater than 1 to emphasize exploration and let the WOA to search the whole search space.

3 AWK-TIS Algorithm

In this section, the main steps of the proposed method are introduced. Firstly, the WOA-Kriging model is constructed based on the basic Kriging model. Secondly, the AWK-TIS method is developed.

3.1 WOA-Kriging Model

In the proposed WOA-Kriging model, the optimal value of correlation parameter θ^* is calculated by integrating WOA into the basic Kriging model. The pattern search method is adopted to seek θ^* in DACE. However, the pattern search method is a local optimization algorithm that needs an initial

solution to search the optimal and it is easy to get trapped in the local optimum. Alternatively, while seeking θ^* , as an efficient global optimization algorithm not depend on the initial solution. WOA is embedded in the DACE toolbox to solve Eq. (8), instead of pattern search algorithm. Then, in our implementations the fitness function for the MLE according to the correlation parameter θ is to minimize the function below [45]:

$$\begin{aligned} \text{Minimize: } & \phi(\theta) = |\mathbf{R}|^{1/m} \hat{\sigma}_z^2 \\ \text{Subject to: } & \theta_k > 0, k = 1, 2, \dots, n \end{aligned} \quad (24)$$

Given the fitness function above, the finding process of θ^* becomes a typical minimization problem. Thus, the population (whale positions) is firstly initialized in a n -dimensional search space, and the population size is set to 25 in this study. Each position corresponds to a correlation parameter vector. Next, a set of mathematical rules in WOA such as encircling prey, spiral bubble-net feeding and search for prey are repeatedly conducted at each iteration. Then, the fitness values of every population are obtained, the fittest solution is ascertained. Finally, the global optimal correlation parameter is acquired until the satisfaction of the stopping criteria that is the maximum number of iterations equals to 100. The main WOA parameters are unchanged during the optimization procedure. Consequently, the WOA-Kriging model is constructed by the optimal correlation parameter θ^* .

3.2 The AWK-TIS Algorithm

In this subsection, the AWK-TIS algorithm is introduced in detail. In AWK-TIS, the real limit state function is substituted by a WOA-Kriging model; the failure probability and its coefficient of variation are computed by TIS method in an active learning way. AWK-TIS mainly consists of three components. Firstly, a WOA-Kriging model is constructed according to the optimal parameter θ^* searched by WOA and the DOE generated through Latin Hypercube Sampling method in the entire design space. Secondly, MPP is evaluated by WOA and the evaluation process is treated as solving a constrained optimization. Thirdly, the active learning method and TIS are adopted together to conduct the selection of the best next sample and the evaluation of the probability. At this stage, the WOA-Kriging model is updated according to the enriched DOE. The general sketch of the AWK-TIS is shown in Fig. 2, and the detailed procedure is proposed as follows:

Step 1: Generation of the initial DOE. Latin Hypercube Sampling (LHS) method is employed to generate the initial samples in the whole design space. Then, the structural response or the real limit state function of every initial sample is evaluated. Thus, the initial DOE is composed of the initial samples and their corresponding responses. The number of the initial samples has an effect on the accuracy of the WOA-Kriging model; however, there are no certain rules to certificate this number.

Step 2: Construction of the WOA-Kriging model. Construct the WOA-Kriging based on initial DOE by embedding WOA to DACE toolbox to find the optimal parameter θ^* . Calculating θ^* will spend a little more computing time, but it is worth since the time consumed for finding accurate parameters could be ignored compared with that for time-consuming simulations. The initial value of θ is unnecessary in this metamodel construction, and the correlation function is chosen to be the Gaussian function.

Step 3: Evaluation of the MPP. The WOA is utilized to calculate the MPP. The notion of reliability index β , is the minimum distance from the origin to the limit state surface in the standard normal space. The reliability index can be therefore calculated as the following constrained optimization problem [9,47,48]:

$$\text{Minimize: } \beta = \min \sqrt{\sum_{i=1}^n (x_i^*)^2} = \min \sqrt{\sum_{i=1}^n [(x_i - \mu_{x_i})/\sigma_{x_i}]^2} \tag{25}$$

Subject to: $\hat{G}(\mathbf{x}) = 0$

where \mathbf{x} denotes the vector of random variants, which is $\mathbf{x} = (x_1, x_2, \dots, x_n)$; x_i^* denotes the standard normal variants; μ_{x_i} and σ_{x_i} represent the mean and standard deviation of the random variant x_i , respectively. $\hat{G}(\mathbf{x})$ is the limit state function constructed by WOA-Kriging model.

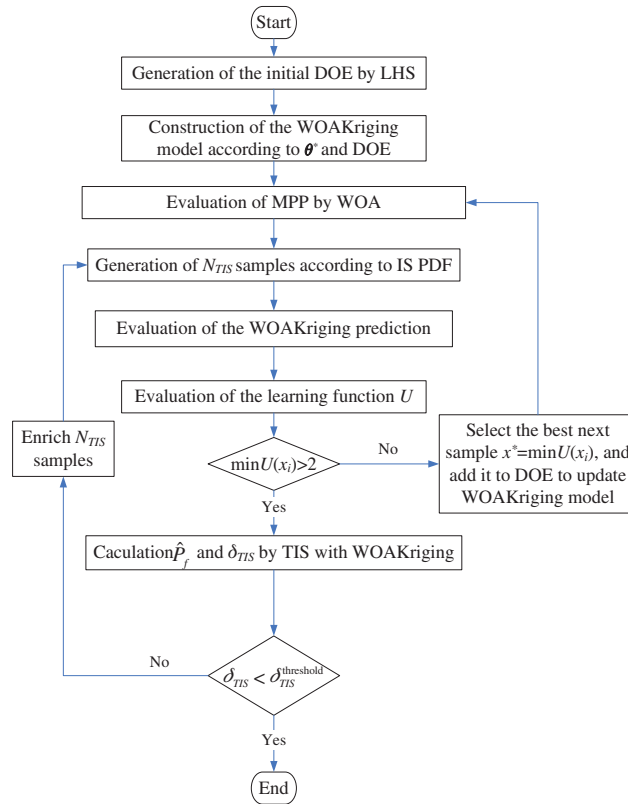


Figure 2: General sketch of the AWK-TIS algorithm

The problem in Eq. (25) is a constrained nonlinear optimization problem. The aim of constraint optimization is to search for feasible solutions with better objective values. However, constrained optimization problems are difficult to solve than unconstrained optimization problems due to the presence of constraints and their interrelationship between the objective functions. As a result, the main assignment while solving the constrained optimization problem is to deal with the constraints.

Step 3.1: Construction of unconstrained function

To avoid the violation of constraints, unfeasible solutions should be adapted to feasible solutions. In the meta-heuristic community, the most common technique is to take advantage of penalty functions to handle these constraints. Thus, a penalty function is employed to convert the constrained

optimization problem in Eq. (25) to the unconstrained one in Eq. (26) [21]:

$$\beta = \min \sqrt{F(\mathbf{x}^*)} = \min \sqrt{\sum_{i=1}^n (x_i^*)^2 + \lambda \hat{G}(\mathbf{x})^2} \quad (26)$$

where, λ is the positive penalty coefficient, and its initial value is set to 10^3 in this paper.

Step 3.2: Calculation of reliability index by WOA

The WOA is adopted to solve the unconstrained function. The inner loop is to find the optimal solution of the Eq. (26) by WOA, while the outer loop is to make sure that the reliability index β is accurate enough. Thus, two stop criteria should be satisfied simultaneously as follows. First, the relative error between the reliability indices in two subsequent outer loop iterations is acceptable [47]:

$$|\beta^{k+1} - \beta^k| / \beta^k < \zeta \quad (27)$$

where k and $k + 1$ indicate the k -th and $k + 1$ -th iteration in the outer loop, respectively, and relative error ζ is a small constant (e.g., 0.01).

Second, it is required that the value of the WOA-Kriging model at the “potential” MPP should be relatively small which means that the “potential” MPP is rather close to the LSF [48]:

$$\lambda \hat{G}(\mathbf{x})^2 \leq \chi \quad (28)$$

where χ is the threshold which is also a small constant (e.g., 0.0001).

If the two criteria above are met simultaneously, the MPP is acquired; otherwise, let $\lambda = 10\lambda$ and go back to Step 3.1. It is noted that in this step the parameters in WOA are remain the same as its original version.

Step 4: *Generation of N_{IS} samples.* N_{IS} samples are generated according to importance sampling density function centered on the MPP found by Step 3. The response of those samples will be evaluated by WOA-Kriging if the active learning procedure requires it.

Step 5: *Conduction of the active learning procedure.* Add $\{x^u, G(x^u)\}$ into the DOE set to rebuild the WOA-Kriging model, and evaluate the learning function U among N_{IS} samples. The learning process continues until the stop criterion, i.e., $\min(U(x_i)) > 2$ is satisfied, which means that the probability of making wrong sign estimation should not exceed 2.3%.

Step 6: *Evaluation of the failure probability and the coefficient of variation δ_{TIS} .* After the WOA-Kriging metamodel is constructed by the active learning method, the next step is to adopt TIS to analyze the reliability. The failure probability and the coefficient of variation are estimated δ_{TIS} by Eqs. (15) and (17), respectively, and make sure that the δ_{TIS} satisfies the predefined threshold. If δ_{TIS} does not satisfy the threshold, a set of new N_{IS} samples are generated to enrich the original N_{IS} samples. In this paper, the threshold of the δ_{TIS} is taken as 0.05.

Step 7: *Output the unbiased estimation of the failure probability.* If δ_{TIS} satisfies the threshold, i.e., $\delta_{TIS} \leq 0.05$ then AWK-TIS terminates, and the failure probability is acquired.

4 Validation Cases

In this section, the efficiency of AWK-TIS is illustrated by four numerical cases and one engineering case. Each of the cases in this study has only a single failure region, which means only one MPP in each case. All the case results are averaged over 10 different runs. The accuracy and efficiency of different algorithms is compared according to the number of calls to the LSF (N_{call}),

δ_{pf} (the coefficient of variation of failure probability) and ε_{pf} (the relative percentage error of failure probability in comparison with the reference value).

4.1 Case 1: 2D Application

A 2D numerical case, which has two independent random variables with standard normal distribution, is chosen to illustrate the process of the proposed method. The limit state function reads

$$G(\mathbf{u}) = 0.5(u_1 - 2)^2 - 1.5(u_2 - 5)^3 - 3 \quad (29)$$

In the proposed method, an initial Kriging model is constructed based on 12 samples within the domain of $[\pm 6]$ in \mathbf{u} space. The results of different methods are summarized in Table 1. The proposed method AWK-TIS is compared with AK-IS, MetaAK-IS², AK-SS. The reference value evaluated by MCS with 5×10^7 samples is taken from [37], and the value is 2.85×10^{-5} . In order to test the robustness of AWK-TIS, 10 different runs are performed with $N_{IS} = 1 \times 10^5$ initial samples centered on the MPP confirmed by WOA. According to N_{call} , i.e., the number of calls to the LSF, the proposed AWK-TIS outperforms the majority of active learning Kriging-based methods except for AK-SS; however, the δ_{pf} , i.e., the coefficient of variation of failure probability of AK-SS is higher than that of AWK-TIS.

Table 1: Results of the 2D application: Case 1

Method	N_{call}	P_f	δ_{pf} (%)	ε_{pf} (%)
MCS [37]	5×10^7	2.85×10^{-5}	2.64	—
AK-IS [37]	19 + 7	2.86×10^{-5}	2.39	0.351
AK-SS [38]	12 + 7	2.85×10^{-5}	9.76	0
MetaAK-IS ² [53]	24 + 4	2.87×10^{-5}	2.39	0.702
AWK-TIS	12 + 9	2.854×10^{-5}	0.78	0.140

Furtherly, the approximation process of the limit state function is schematically illustrated in Fig. 3, including LSF (green line), Kriging model (red dotted line), initial samples (black fork dots), added samples (pink circle) and MPP (blue hexagon). Moreover, the MPP searched by WOA is located almost in the same position after 5 iterations while the enriched DOE are updated sequentially by U learning function. The convergence process of failure probability P_f and the C.O.V of P_f for AWK-TIS are presented in Fig. 4.

It can be seen from Figs. 3 and 4 that these newly computed samples are located in the vicinity of the limit state function and are used to improve the accuracy of Kriging metamodel. Moreover, AWK-TIS requires much less performance function computations than AK-IS. Indeed, AWK-TIS needs 9 computations of real limit state function after the construction of Kriging model by initial DOE.

As described in Section 2.4, the WOA is adopted to acquire the correlation parameter θ . The number of search agents is 25, the number of iterations is set to 100, and other parameters in WOA are remaining as the original form. Fig. 5 depicts the convergence of the Kriging correlation parameter θ shown in Eq. (8) when the update process of the WOA-Kriging model is stopped. Moreover, Fig. 5 shows that the maximum likelihood estimation of θ convergence to the minimum value of 6.49×10^{-6} at the 16th iteration, and the optimum θ is found at this point. Compared with PSO and GA, the WOA shows its high convergence speed and calculation accuracy.

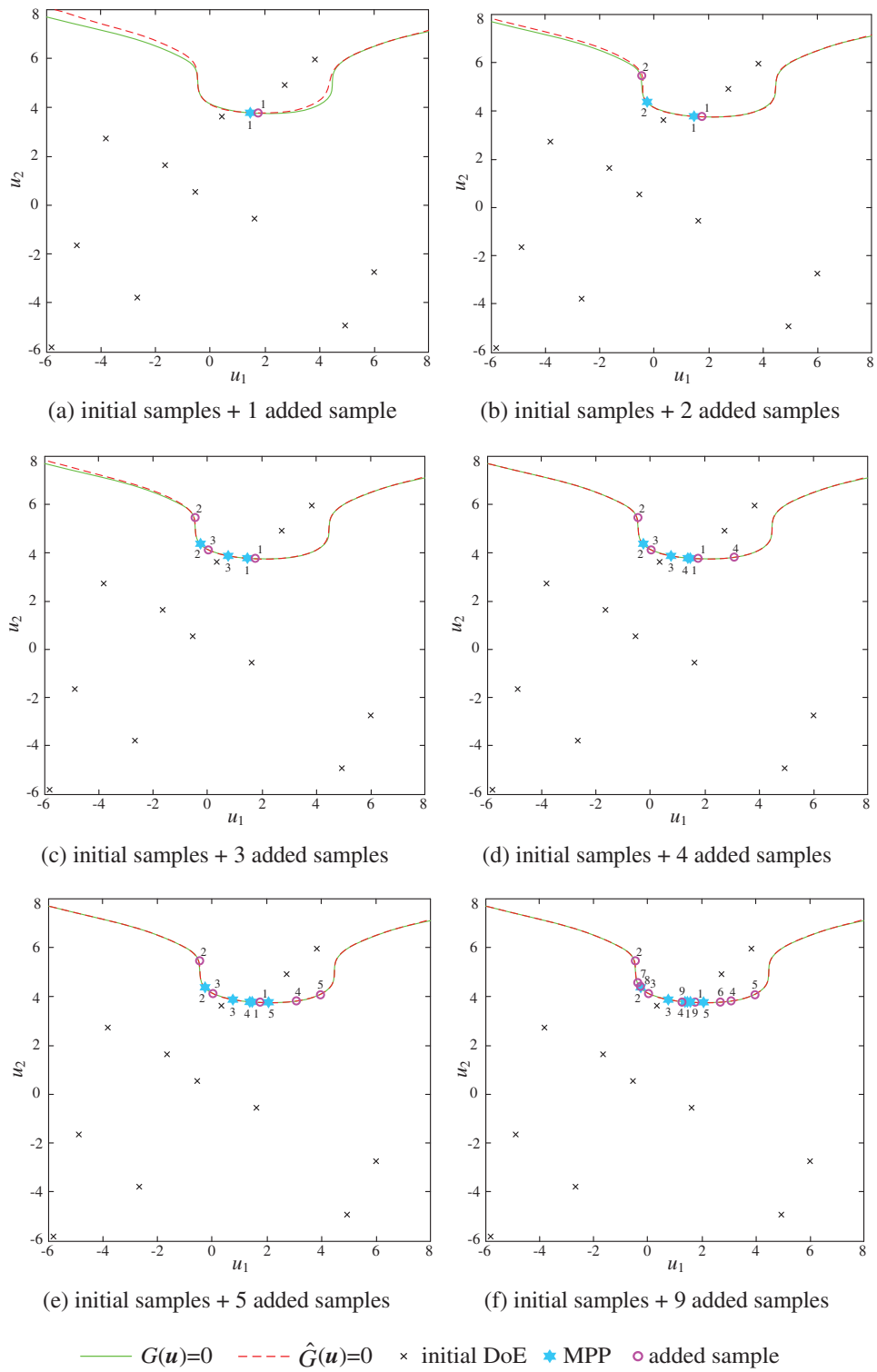


Figure 3: The approximation process of the LSF for case 1

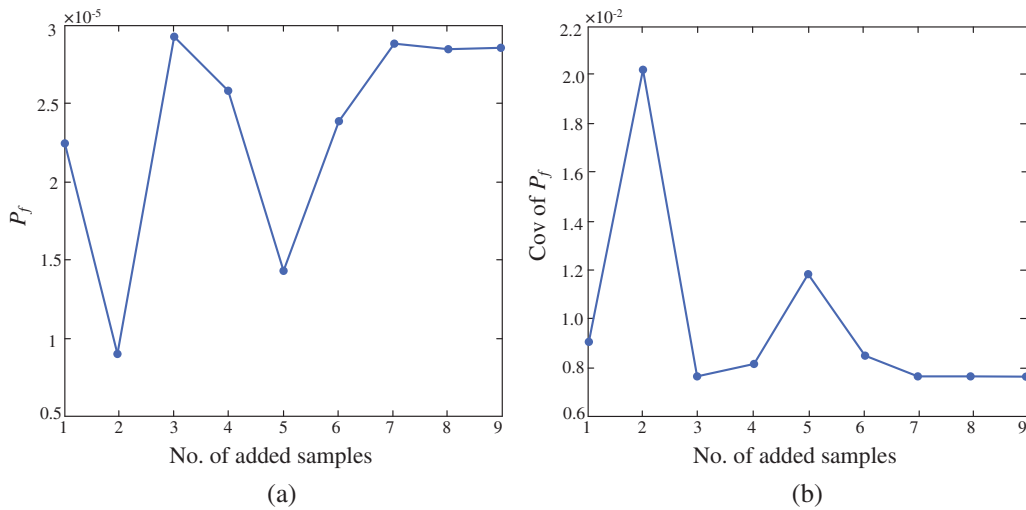


Figure 4: Convergence process of P_f and C.O.V of P_f for case 1

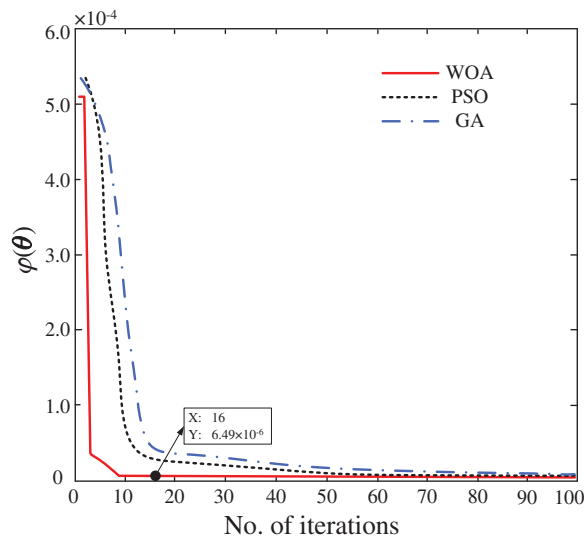


Figure 5: The process to find θ^* using WOA for case 1

4.2 Case 2: A Cantilever Beam Example

This case has been widely used in literature [38]. The cantilever beam, which has a rectangular cross-section, is subjected to a distributed uniform load. The limit state function which is defined by the maximum vertical displacement of the beam is given as

$$G(\mathbf{x}) = 0.01846154 - 74.76923x_1/x_2^3 \tag{30}$$

where x_1 and x_2 are assumed to be independent random variables following normal distribution. The statistical properties of the above two variables are shown in Table 2. The results obtained by the proposed AWK-TIS, MSC, AK-MCS, and AK-SS are listed in Table 3.

Table 2: Statistical properties of the variables for case 2

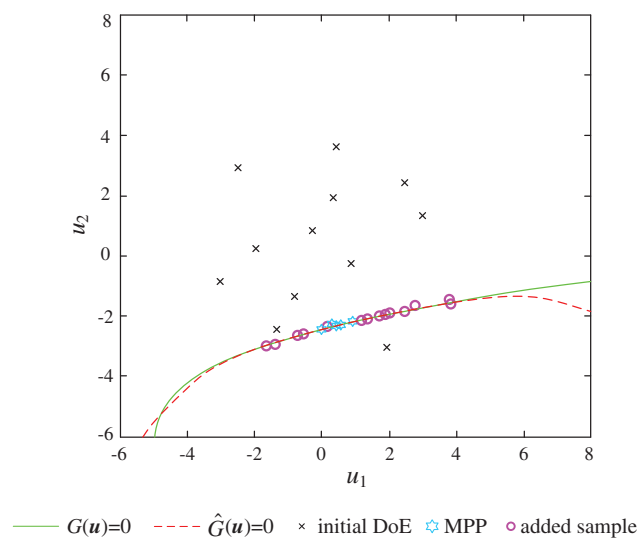
Variable	Mean	Variation coefficient	Distribution
x_1	1000 Mpa	0.2	Normal
x_2	250 mm	0.15	Normal

Table 3: Results of case 2

Method	N_{call}	P_f	δ_{P_f} (%)	ε_{P_f} (%)
MCS [38]	1×10^6	9.51×10^{-3}	1.02	—
AK-MCS [38]	33	9.52×10^{-3}	4.63	0.105
AK-SS [38]	28	9.51×10^{-3}	4.92	0
AWK-TIS	12 + 16	9.525×10^{-3}	0.58	0.157

From Table 3, it can be seen that the N_{call} of the proposed AWK-TIS is the same as that of AK-SS, but it is less than the number of samples applied in AK-MCS. Besides, the one can see that all the P_f calculated by the different methods have high accuracy comparing with the MCS solution. However, the coefficient of variation of failure probability of AWK-TIS is the smallest in the four methods.

Similarly to Figs. 3 and 4, Fig. 6 shows the final approximation of AWK-TIS and Fig. 7 shows the convergence process of failure probability and the C.O.V of failure probability. As shown in Fig. 6, the added samples are almost in the vicinity of the real LSF, and the LSF constructed by Kriging can be accurately approximated in the domain of the sampling region. On the contrary, the Kriging model shows inexact outside the sampling region. Nevertheless, it should be indicated that the region outside the sampling area has little influence on the failure probability calculation due to the MPP is far away from this area. From Fig. 7, the proposed method has converged to the final results at about 12 added samples, which indicates the efficiency and accuracy of the AWK-TIS.

**Figure 6:** The approximation of the LSF for case 2

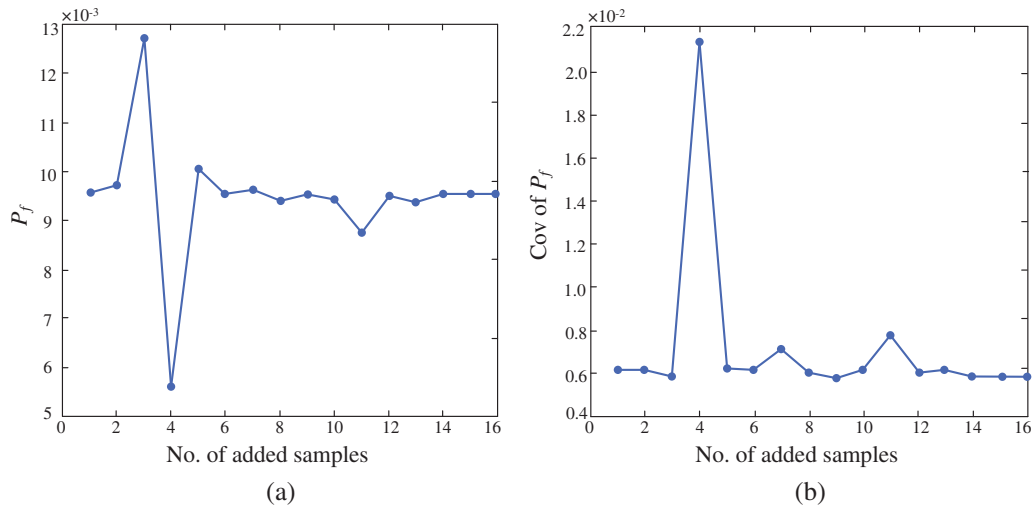


Figure 7: Convergence process of P_f and C.O.V of P_f for case 2

4.3 Case 3: A Non-Linear Oscillator

A non-linear undamped single degree of freedom system depicted in Fig. 8 is analyzed in this case. The limit state function is given as [54]

$$G(C_1, C_2, M, R, T_1, F_1) = 3R - \left| \frac{2F_1}{M\omega_0^2} \sin\left(\frac{\omega_0 T_1}{2}\right) \right| \tag{31}$$

where $\omega_0 = \sqrt{(C_1 + C_2)/M}$. Six random input variables including C_1 , C_2 , M , R , T_1 , and F_1 are listed in Table 4. The initial number of DOE is set as 20. The AWK-TIS is compared with several other existing methods (MCS, AK-MCS, PAK-Bⁿ [54]) and their results are listed in Table 5. Same as the two cases above, the reference values to compare the reliability analysis results are the P_f , C.O.V of P_f , δ_{P_f} , ε_{P_f} , estimated by MCS.

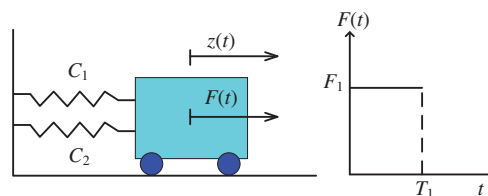


Figure 8: A non-linear oscillator

Table 4: Statistical properties of the variables for case 3

Variable	Mean	Standard deviation	Distribution
M	1	0.05	Normal
C_1	1	0.1	Normal
C_2	0.1	0.1	Normal
R	0.5	0.1	Normal

(Continued)

Table 4 (continued)

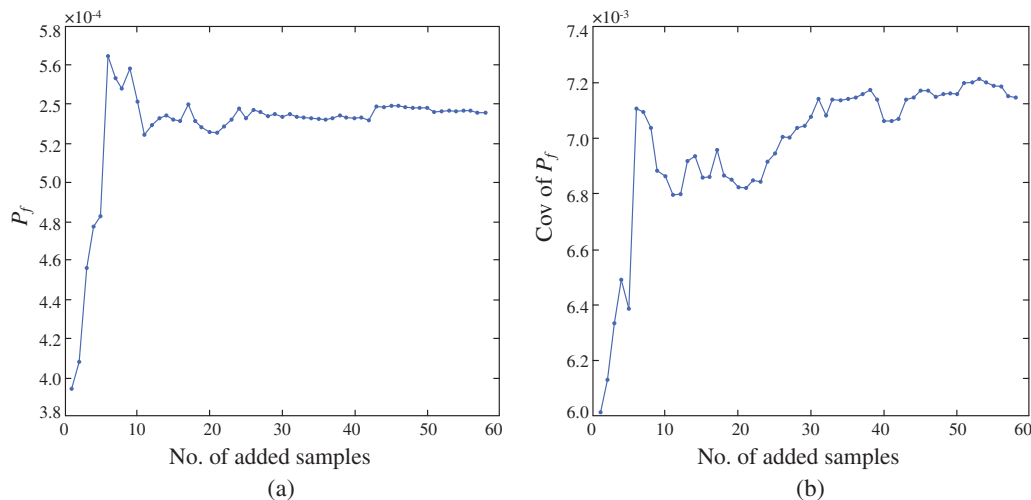
Variable	Mean	Standard deviation	Distribution
T_1	1	0.2	Normal
F_1	0.6	0.2	Normal

Table 5: Results of case 3

Method	N_{call}	P_f	δ_{P_f} (%)	ε_{P_f} (%)
MCS [54]	1.0×10^6	5.46×10^{-4}	4.28	—
AK-MCS [54]	>300	5.49×10^{-4}	4.81	0.549
PAK-B ⁿ [54]	20 + 106	5.50×10^{-4}	4.78	0.732
AWK-TIS	20 + 59	5.36×10^{-4}	0.071	1.832

It can be seen from Table 5 that although the relative error of failure probability obtained by the proposed method is slightly larger than that of AK-MCS and PAK-Bⁿ, the N_{call} of AWK-TIS is significantly reduced contrasted with that of the two methods above. Additionally, the C.O.V of failure probability is rather small compared with the other three methods. Hence, it indicates that AWK-TIS could solve the problem of small failure probability with a moderate number of random variables.

Equally, Fig. 9 presents the convergence process of failure probability and C.O.V of failure probability of this case. From Fig. 9, one can see that the failure probability has converged with almost 50 added samples, which means that the proposed AWK-TIS is suitable for the calculation of the small failure probability.

**Figure 9: Convergence process of P_f and C.O.V of P_f for case 3**

4.4 Case 4: A Roof Truss Structure

A roof truss structure, which is selected to verify the proposed method, is shown in Fig. 10. The roof truss undertaking the uniformly distributed load q that can be converted to the nodal load

$P = ql/4$. The response of the roof truss is the perpendicular deflection ΔC of node C is denoted as [55]:

$$\Delta C = \frac{q l^2}{2} \left(\frac{3.81}{A_c E_c} + \frac{1.13}{A_s E_s} \right) \tag{32}$$

where A_c, A_s, E_c, E_s respectively are sectional area, elastic modulus concrete and steel bars, l is the length of the structure. The mean and variation coefficient of the six independent normal distribution random variables are reported in Table 6. The threshold of ΔC should not be larger than 0.03 m, and the LSF of this case is thus defined as

$$G(\mathbf{x}) = 0.03 - \Delta C \tag{33}$$

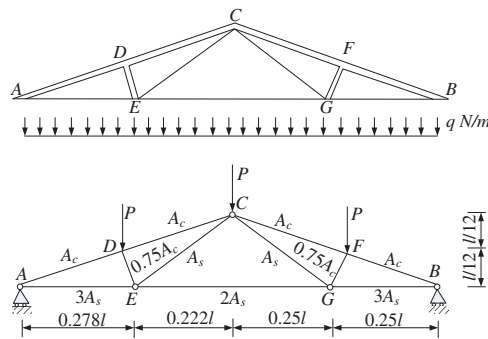


Figure 10: The schematic diagram of a roof truss

Table 6: Statistical properties of the variables for case 3

Variable	Mean	Variation coefficient	Unit
q	2×10^4	0.07	N/m
l	12	0.01	m
A_s	9.82×10^{-4}	0.06	m ²
A_c	0.04	0.12	m ²
E_s	1×10^{11}	0.06	N/m ²
E_c	2×10^{10}	0.06	N/m ²

The AWK-TIS is compared with other existing methods (MCS, AK-MCS, KAIS, RBF) and the results are summarized in Table 7. The results by MCS calculations with 1.06×10^6 samples are regarded as reference values in this case.

Table 7: Results of case 4

Method	N_{call}	P_f	δ_{P_f}	ε_{P_f} (%)
MCS [55]	1.06×10^6	9.395×10^{-3}	0.01	—
AK-MCS [55]	12 + 255	9.460×10^{-3}	0.05	0.692
KAIS [55]	28 + 72 + 115	9.365×10^{-3}	0.05	0.319

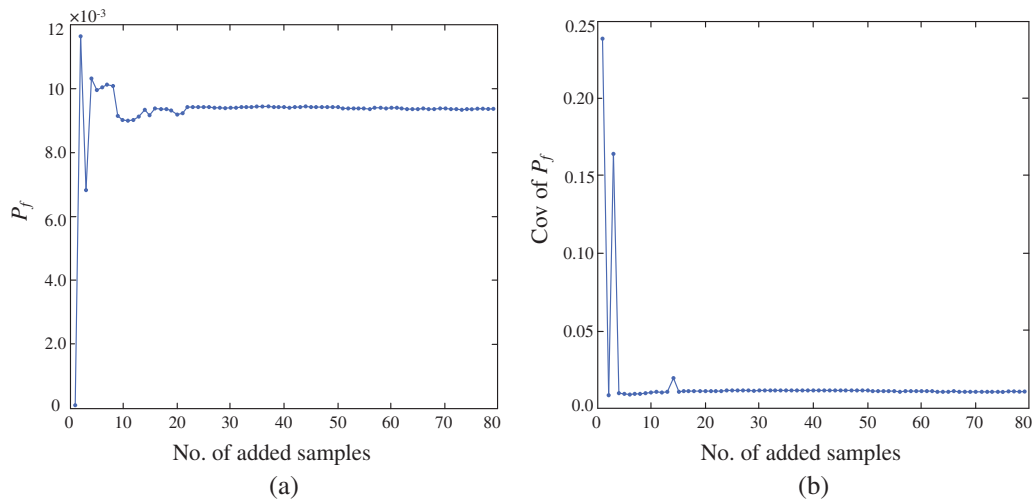
(Continued)

Table 7 (continued)

Method	N_{call}	P_f	δ_{P_f}	ε_{P_f} (%)
RBF [25]	12 + 143	9.736×10^{-3}	/	3.629
AWK-TIS	20 + 79	9.357×10^{-3}	0.01	0.404

It can be seen from Table 7 that AWK-TIS needs only 99 N_{call} to acquire a satisfactory result while the other three approaches demand more than 150 N_{call} . The small N_{call} has highlighted the numerical efficiency of the proposed approach in estimating the roof truss structure. Furthermore, the AWK-TIS has the second relative error of 0.404% comparing with the reference value of P_f evaluated by MCS, followed by AK-MCS and RBF.

By investigating the convergence process of P_f and C.O.V of P_f presented in Fig. 11, we can see that both of the curves converged at about 25 added samples, which means that the proposed AWK-TIS is suitable for dealing with small failure probabilities and relatively large number of random variables. Additionally, the convergence threshold can be advisably loosed to further improve computational efficiency.

**Figure 11:** Convergence process of P_f and C.O.V of P_f for case 4

4.5 Case 5: A Jet Vane Manipulation Mechanism

Vertical launch missile is widely used on land air defense and sea air defense. The performance of a jet vane system is extremely vital to the flying control of vertical launch missile. As a significant component of the jet van system, the manipulation mechanism drives the rudder rotating in the engine gas flow that generates pitch moment to control the orientation of the missile, which is shown in Fig. 12a. The manipulate mechanism converts the linear motion of the servo motor to the rotation of the jet van, and the schematic of this mechanism is shown in Fig. 12b.

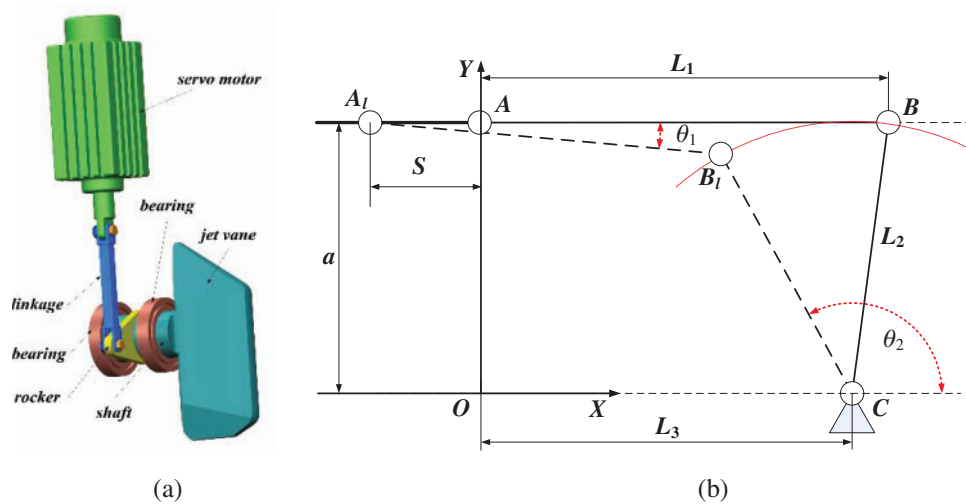


Figure 12: A jet van manipulation mechanism

In Fig. 12b, A and B represent the positions of the two ends of the linkage respectively, and C is the center of the shaft. L_1 and L_2 are the length of linkage and rocker respectively. L_3 is the distance between A and C along the X -axial. a is the distance between A and C . S is the maximum displacement of A along the negative direction of X -axial, and A_1, B_1 are the left limit position of the linkage. θ_2 is the angle between the BC and the X -axial, and it is the function of L_1, L_2, L_3, a and S , which is shown in Eq. (34)

$$\theta_2 = \pi - \arctan \left(\frac{a - L_1 \sin \theta_1}{L_3 - S - L_1 \cos \theta_1} \right) \tag{34}$$

where θ_1 is the angle between the linkage and the X -axial.

In this case, the linkage length L_1 , the length of the rocker L_2 , the distance between A and C along the X -axial L_3 , and the maximum displacement of linear servo system S are taken as random variables. Table 8 lists the details of random variables. To assure the normal operation of the manipulation mechanism, the maximum angle of the rudder shaft should not exceed a given threshold. Therefore, the limit state function is defined as

$$G(\mathbf{X}) = \theta_m - \theta_2(\mathbf{X}) \tag{35}$$

where θ_m is the threshold of the maximum angle of the rudder shaft which is taken as 118.2° , $\theta_2(\mathbf{X})$ is the maximum angle of the rudder shaft which is calculated by solving Eq. (34), the \mathbf{X} represents all the random variables.

Table 8: Statistical properties of the variables for case 5

Variable	Mean	Standard deviation	Unit
L_1	82	0.017	mm
L_2	42	0.033	mm
L_3	80.5	0.033	mm
S	21	0.033	mm

The results of the different methods are shown in Table 9, in which results estimated by the AK-MCS and AK-IS methods are also provided for the sake of comparison. Besides, the calculation times or CPU-time of different AK-based algorithm are also exhibited in this table. The sample pool of the MCS, AK-MCS and AK-IS are 5×10^7 , 5×10^6 and 4×10^6 , respectively.

Table 9: Results of the case 5

Method	N_{call}	P_f	δ_{P_f} (%)	ε_{P_f} (%)	CPU-time (s)
MCS	5×10^7	8.384×10^{-5}	1.543	—	/
AK-MCS	45	8.580×10^{-5}	4.828	2.337	70.311
AK-IS	8 + 34	8.799×10^{-5}	4.933	4.949	84.258
AWK-TIS	12 + 24	8.325×10^{-5}	0.585	0.704	80.624

Table 9 shows that the predictive accuracy of the AWK-TIS notably outperforms the other two AK methods considering the relative error of failure probability. Besides, the N_{call} is less than that of AK-MCS and AK-IS, which indicates that the proposed AWK-TIS can solve real engineering problem efficiently. From the CPU-time results, it is concluded that although the process of optimizing Kriging model by WOA algorithm additionally increases the computational time, the utilization of the TIS method reduces the calculation time.

The convergence of failure probability and coefficient of variation of failure probability is presented in Fig. 13. From Fig. 13, the P_f and C.O.V of P_f have converged to the final results at about the 10 added samples. Thus, the computational performance of the AWK-TIS when dealing with this case can be improved with a loose stopping criterion.

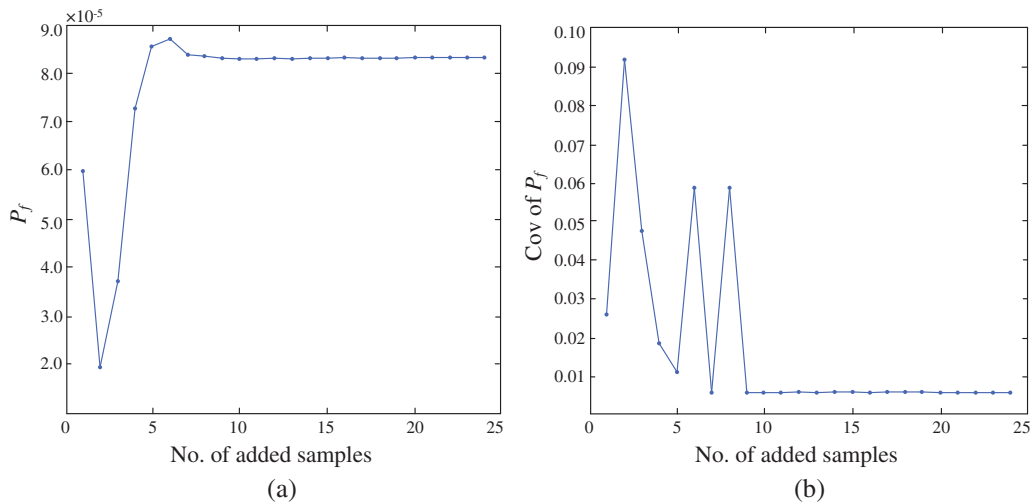


Figure 13: Convergence process of P_f and C.O.V of P_f for case 5

5 Conclusions

The AWK-TIS method is proposed as a novel reliability method to deal with structural reliability problems, in which the WOA is performed to seek the optimum correlation parameter of Kriging

model and the MPP, and then the added samples generated by U learning function are enriched to DOE to refine the Kriging model. The MPP is calculated by WOA through solving the constrained nonlinear optimization problem until certain two thresholds are satisfied simultaneously. Afterward, the TIS method is applied to calculate the failure probability and coefficient of variation of the failure probability. In AWK-TIS, the sample pool is much smaller than that of AK-IS, which significantly expedites the learning efficiency. Five test cases including four numerical cases and one engineering case are adopted to verify the performance of the AWK-TIS method. Results prove that the proposed method can achieve high computational accuracy and efficiency.

AWK-TIS method has two main drawbacks: (1) AWK-TIS, like AK-IS, is dependent on the MPP to ensure the next best point; however, the solitary sampling center has confined its employment in dealing with multi-MPP problems, (2) the process of acquiring the MPP is transformed to solve the constrained nonlinear optimization problem, which may affect the efficiency of the proposed method, (3) due to the restriction of IS-based algorithm, the proposed algorithm does have some defects in dealing with high-dimensional problems. Future works will focus on three aspects: (1) adopt other efficient sampling methods in lieu of TIS to solve multi-MPP problems, (2) improve the efficiency of WOA by hybridising other optimizers or employing other more effective optimization algorithms to solve the constrained optimization problem to obtain the MPP, (3) alternative modeling and analysis methods need to be incorporated for effective validation of AWK-TIS to high-dimensional problems.

Funding Statement: This work is supported by the Technical Basic Scientific Research Projects of State Administration of Science, Technology and Industry for National Defence, PRC (Grant No. JSZL2019204C001).

Conflicts of Interest: The authors declare that they have no conflicts of interest to report regarding the present study.

References

1. Guimarães, H., Matos, J. C., Henriques, A. A. (2018). An innovative adaptive sparse response surface method for structural reliability analysis. *Structural Safety*, 73, 12–28. DOI 10.1016/j.strusafe.2018.02.001.
2. Moustapha, M., Marelli, S., Sudret, B. (2022). Active learning for structural reliability: Survey, general framework and benchmark. *Structural Safety*, 96, 102174. DOI 10.1016/j.strusafe.2021.102174.
3. Li, H. S., Cao, Z. J. (2016). Matlab codes of subset simulation for reliability analysis and structural optimization. *Structural and Multidisciplinary Optimization*, 54, 1–20. DOI 10.1007/s00158-016-1414-5.
4. Zhang, J. H., Xiao, M., Gao, L. (2019). An active learning reliability method combining Kriging constructed with exploration and exploitation of failure region and subset simulation. *Reliability Engineering and System Safety*, 188, 90–102. DOI 10.1016/j.ress.2019.03.002.
5. Thedy, J., Liao, K. W. (2021). Multisphere-based importance sampling for structural reliability. *Structural Safety*, 91, 102099. DOI 10.1016/j.strusafe.2021.102099.
6. Pan, Q. J., Zhang, R. F., Ye, X. Y., Li, Z. W. (2021). An efficient method combining polynomial-chaos kriging and adaptive radial-based importance sampling for reliability analysis. *Computers and Geotechnics*, 140, 104434. DOI 10.1016/j.compgeo.2021.104434.
7. Shayanfar, M. A., Barkhordari, M. A., Barkhori, M., Barkhori, M. (2018). An adaptive directional importance sampling method for structural reliability analysis. *Structural Safety*, 70, 14–20. DOI 10.1016/j.strusafe.2017.07.006.

8. Guo, Q., Liu, Y. S., Chen, B. Q., Zhao, Y. Z. (2020). An active learning Kriging model combined with directional importance sampling method for efficient reliability analysis. *Probabilistic Engineering Mechanics*, 60, 103054. DOI 10.1016/j.probengmech.2020.103054.
9. Zhu, S. P., Keshtegar, B., Trung, N. T., Yaseen, Z. M., Bui, D. T. (2021). Reliability-based structural design optimization: Hybridized conjugate mean value approach. *Engineering with Computers*, 37(1), 381–394. DOI 10.1007/s00366-019-00829-7.
10. Zhu, S. P., Liu, Q., Peng, W. W., Zhang, X. C. (2018). Computational-experimental approaches for fatigue reliability assessment of turbine bladed disks. *International Journal of Mechanical Sciences*, 142–143, 502–517. DOI 10.1016/j.ijmecsci.2018.04.050.
11. Zhu, S. P., Keshtegar, B., Ben, S., Mohamed El, A. B., Zio, E. et al. (2022). Hybrid and enhanced PSO: Novel first order reliability method-based hybrid intelligent approaches. *Computer Methods in Applied Mechanics and Engineering*, 393, 114730. DOI 10.1016/j.cma.2022.114730.
12. Zhu, S. P., Keshtegar, B., Bagheri, M., Hao, P., Trung, N. T. (2020). Novel hybrid robust method for uncertain reliability analysis using finite conjugate map. *Computer Methods in Applied Mechanics and Engineering*, 371, 113309. DOI 10.1016/j.cma.2020.113309.
13. Li, X. Q., Song, L. K., Bai, G. C. (2022). Recent advances in reliability analysis of aeroengine rotor system: A review. *International Journal of Structural Integrity*, 13(1), 1–29. DOI 10.1108/IJSI-10-2021-0111.
14. Wang, Y. H., Zhang, C., Su, Y. Q., Shang, L. Y., Zhang, T. (2020). Structure optimization of the frame based on response surface method. *International Journal of Structural Integrity*, 11(3), 411–425. DOI 10.1108/IJSI-07-2019-0067.
15. Zhi, P., Xu, Y., Chen, B. (2020). Time-dependent reliability analysis of the motor hanger for EMU based on stochastic process. *International Journal of Structural Integrity*, 11(3), 453–469. DOI 10.1108/IJSI-07-2019-0075.
16. Zhu, S. P., Liu, Q., Zhou, J., Yu, Z. Y. (2018). Fatigue reliability assessment of turbine discs under multi-source uncertainties. *Fatigue & Fracture of Engineering Materials & Structures*, 41(6), 1291–1305. DOI 10.1111/ffe.12772.
17. Lim, H., Manuel, L. (2021). Distribution-free polynomial chaos expansion surrogate models for efficient structural reliability analysis. *Reliability Engineering and System Safety*, 205, 107256. DOI 10.1016/j.ress.2020.107256.
18. Qin, Q., Feng, Y. W., Li, F. (2018). Structural reliability analysis using enhanced cuckoo search algorithm and artificial neural network. *Journal of Systems Engineering and Electronics*, 29(6), 1317–1326. DOI 10.21629/JSEE.2018.06.19.
19. Deng, J., Gu, D., Li, X. (2005). Structural reliability analysis for implicit performance functions using artificial neural network. *Structural Safety*, 27, 25–48. DOI 10.1016/j.strusafe.2004.03.004.
20. Zhao, H. B., Li, S. J., Ru, Z. L. (2017). Adaptive reliability analysis based on a support vector machine and its application to rock engineering. *Applied Mathematical Modelling*, 44, 508–522. DOI 10.1016/j.apm.2017.02.020.
21. Cheng, K., Lu, Z. Z. (2021). Adaptive Bayesian support vector regression model for structural reliability analysis. *Reliability Engineering and System Safety*, 206, 107286. DOI 10.1016/j.ress.2020.107286.
22. Tan, X. H., Bi, W. H., Hou, X. L. (2011). Reliability analysis using radial basis function networks and support vector machines. *Computers and Geotechnics*, 38, 178–186. DOI 10.1016/j.compgeo.2010.11.002.
23. Li, X., Gong, C. L., Gu, L. X., Gao, W. K., Jing, Z. et al. (2018). A sequential surrogate method for reliability analysis based on radial basis function. *Structural Safety*, 73, 42–53. DOI 10.1016/j.strusafe.2018.02.005.
24. Xiao, N. C., Zuo, M. J., Guo, W. (2018). Efficient reliability analysis based on adaptive sequential sampling design and cross-validation. *Applied Mathematical Modelling*, 58, 404–420. DOI 10.1016/j.apm.2018.02.012.

25. Xiong, B., Tan, H. F. (2018). A robust and efficient structural reliability method combining radial-based importance sampling and Kriging. *Science China Technological Sciences*, 61, 724–734. DOI 10.1007/s11431-016-9068-1.
26. Hong, L. X., Li, H. C., Peng, K. (2021). A combined radial basis function and adaptive sequential sampling method for structural reliability analysis. *Applied Mathematical Modelling*, 90, 375–393. DOI 10.1016/j.apm.2020.08.042.
27. Eason, J., Cremaschi, S. (2014). Adaptive sequential sampling for surrogate model generation with artificial neural networks. *Computers and Chemical Engineering*, 68, 220–232. DOI 10.1016/j.compchemeng.2014.05.021.
28. Bichon, B. J., Eldred, M. S., Swiler, L. P., Mahadevan, S., McFarland, J. M. (2008). Efficient global reliability analysis for nonlinear implicit performance functions. *AIAA Journal*, 46(10), 2459–2468. DOI 10.2514/1.34321.
29. Echard, B., Gayton, N., Lemaire, M. (2011). AK-MCS: An active learning reliability method combining Kriging and Monte Carlo simulation. *Structural Safety*, 33(2), 145–154. DOI 10.1016/j.strusafe.2011.01.002.
30. Lv, Z. Y., Lu, Z. Z., Wang, P. (2015). A new learning function for Kriging and its applications to solve reliability problems in engineering. *Computers and Math*, 70(5), 1182–1197. DOI 10.1016/j.camwa.2015.07.004.
31. Li, M., Shen, S., Barzegar, V., Sadoughi, M., Hu, C. et al. (2021). Kriging-based reliability analysis considering predictive uncertainty reduction. *Structural and Multidisciplinary Optimization*, 63(6), 2721–2737. DOI 10.1007/s00158-020-02831-w.
32. Sun, Z., Wang, J., Li, R., Tong, C. (2017). LIF: A new Kriging based learning function and its application to structural reliability analysis. *Reliability Engineering and System Safety*, 157, 152–165. DOI 10.1016/j.res.2016.09.003.
33. Wen, Z. X., Pei, H. Q., Liu, H., Yue, Z. F. (2016). A sequential Kriging reliability analysis method with characteristics of adaptive sampling regions and parallelizability. *Reliability Engineering and System Safety*, 153, 170–179. DOI 10.1016/j.res.2016.05.002.
34. Zhang, X. F., Wang, L., Sørensen, J. D. (2019). REIF: A novel active-learning function toward adaptive Kriging surrogate models for structural reliability analysis. *Reliability Engineering and System Safety*, 185, 440–454. DOI 10.1016/j.res.2019.01.014.
35. Xiong, Y., Sampath, S. (2021). A fast-convergence algorithm for reliability analysis based on the AK-MCS. *Reliability Engineering & System Safety*, 213, 107693. DOI 10.1016/j.res.2021.107693.
36. Zhou, T., Peng, Y. B. (2022). Reliability analysis using adaptive polynomial-chaos Kriging and probability density evolution method. *Reliability Engineering & System Safety*, 220, 108283. DOI 10.1016/j.res.2021.108283.
37. Echard, B., Gayton, N., Lemaire, M., Relun, N. (2013). A combined importance sampling and kriging reliability method for small failure probabilities with time-demanding numerical models. *Reliability Engineering and System Safety*, 111, 232–240. DOI 10.1016/j.res.2012.10.008.
38. Huang, X., Chen, J., Zhu, H. (2016). Assessing small failure probabilities by AK-SS: An active learning method combining Kriging and subset simulation. *Structural Safety*, 59, 86–95. DOI 10.1016/j.strusafe.2015.12.003.
39. Zhang, X. B., Lu, Z. Z., Cheng, K. (2021). AK-DS: An adaptive Kriging-based directional sampling method for reliability analysis. *Mechanical Systems and Signal Processing*, 156, 107610. DOI 10.1016/j.ymsp.2021.107610.
40. Zhang, X. F., Wang, L., Sørensen, J. D. (2020). AKOIS: An adaptive Kriging oriented importance sampling method for structural system reliability analysis. *Structural Safety*, 82, 101876. DOI 10.1016/j.strusafe.2019.101876.

41. Yun, W. Y., Lu, Z. Z., Jiang, X., Zhang, L. G., He, P. F. (2020). AK-ARBIS: An improved AK-MCS based on the adaptive radial-based importance sampling for small failure probability. *Structural Safety*, 82, 101891. DOI 10.1016/j.strusafe.2019.101891.
42. Ameryan, A., Ghalehnovi, M., Rashki, M. (2022). AK-SESC: A novel reliability procedure based on the integration of active learning Kriging and sequential space conversion method. *Reliability Engineering and System Safety*, 217, 108036. DOI 10.1016/j.ress.2021.108036.
43. Wang, J. S., Xu, G. J., Li, Y. L., Ahsan, K. (2022). AKSE: A novel adaptive Kriging method combining sampling region scheme and error-based stopping criterion for structural reliability analysis. *Reliability Engineering and System Safety*, 219, 108214. DOI 10.1016/j.ress.2021.108214.
44. Lophaven, S., Nielsen, H., Søndergaard, J. (2002). *DACE a matlab Kriging toolbox*. Denmark: Technical University of Denmark.
45. Lu, C., Feng, Y. W., Liem, R. P., Fei, C. W. (2018). Improved Kriging with extremum response surface method for structural dynamic reliability and sensitivity analyses. *Aerospace Science and Technology*, 76, 164–175. DOI 10.1016/j.ast.2018.02.012.
46. Yang, X. F., Liu, Y. S., Zhang, Y. S., Yue, Z. F. (2015). Probability and convex set hybrid reliability analysis based on active learning Kriging model. *Applied Mathematical Modelling*, 39, 3954–3971. DOI 10.1016/j.apm.2014.12.012.
47. Yi, P., Wei, K. T., Kong, X. J. (2015). Cumulative PSO-Kriging model for slope reliability analysis. *Probabilistic Engineering Mechanics*, 39, 39–45. DOI 10.1016/j.probengmech.2014.12.001.
48. Luo, X., Li, X., Zhou, J. (2012). A Kriging-based hybrid optimization algorithm for slope reliability analysis. *Structural Safety*, 34, 401–406. DOI 10.1016/j.strusafe.2011.09.004.
49. Mirjalili, S., Lewis, A. (2016). The whale optimization algorithm. *Advances in Engineering Software*, 95, 51–67. DOI 10.1016/j.advengsoft.2016.01.008.
50. Jing, Z., Chen, J. Q., Li, X. (2019). RBF-GA: An adaptive radial basis function metamodeling with genetic algorithm for structural reliability analysis. *Reliability Engineering and System Safety*, 189, 42–57. DOI 10.1016/j.ress.2019.03.005.
51. Yun, W. Y., Lu, Z. Z., Jiang, X. (2018). A modified importance sampling method for structural reliability and its global reliability sensitivity analysis. *Structural and Multidisciplinary Optimization*, 57, 1625–1641. DOI 10.1007/s00158-017-1832-z.
52. Grooteman, F. (2008). Adaptive radial-based importance sampling method for structural reliability. *Structural Safety*, 30, 533–542. DOI 10.1016/j.strusafe.2007.10.002.
53. Cadini, F., Santos, F., Zio, E. (2014). An improved adaptive Kriging-based importance technique for sampling multiple failure regions of low probability. *Reliability Engineering and System Safety*, 131, 109–117. DOI 10.1016/j.ress.2014.06.023.
54. Kim, J., Song, J. (2020). Probability-adaptive Kriging in n-ball (PAK-bⁿ) for reliability analysis. *Structural Safety*, 85, 101924. DOI 10.1016/j.strusafe.2020.101924.
55. Zhao, H. L., Yue, Z. F., Liu, Y. S., Gao, Z. Z., Zhang, Y. S. (2015). An efficient reliability method combining adaptive importance sampling and Kriging metamodel. *Applied Mathematical Modelling*, 39, 1853–1866. DOI 10.1016/j.apm.2014.10.015.